

Low Bypass Ratio Turbofan Performance Modelling with Fan Radial Flow Profiles

Man San LI¹, Jun Fei YIN¹, Barry CURNOCK²

¹School of Engineering, Department of Power, Propulsion and Aerospace Engineering,
Cranfield University
Bedfordshire, MK43 0AL, UK

Phone: +44-(0)-1234-750111, ext. 5262, FAX: +44-(0)-1234-752407, E-mail: m.s.li.1999@cranfield.ac.uk

²Rolls-Royce plc, Bristol, UK

ABSTRACT

In gas turbine performance simulation radial profiles of flowpath parameters through the fan component of turbofan engines have traditionally been addressed by using the inner and outer fan model, to achieve more realistic averaged properties of the flow at the downstream components. Fan performance data for engine performance simulation is usually obtained as fan performance characteristic maps by rig testing.

In certain cases, low bypass ratio fans display a behaviour where the overall fan non-dimensional performance is dependent on the operating bypass ratio at a fixed non-dimensional overall flow and corrected speed. A more general fan performance simulation model is described here that involves the modelling of radial profiles. It addresses the deviation from the rig test schedule of bypass ratio versus corrected speed that occurs when simulating the engine with, for example, bleeds, transients and nozzle area changes.

NOMENCLATURE

AHNZ	Hot nozzle area
BPR	Bypass ratio
CFD	Computational fluid dynamics
CN	Relative shaft speed $(N/\sqrt{T_1}) / (N/\sqrt{T_1})_{\text{design pt}}$
H	Total enthalpy
HBPR	High bypass ratio
HPC	High pressure compressor
HPT	High pressure turbine
LBPR	Low bypass ratio
LPT	Low pressure turbine
N	Shaft rotational speed
P	Total pressure
PR	Pressure ratio P_2/P_1
R	Fan rotor radial distance
R _s	Non-dimensional rotor radial distance
SFC	Specific fuel consumption
SLS	Sea-level static
T	Total temperature
TET	Turbine entry total temperature
W	Total fan mass flow
W_{R_s}	Cumulative mass flow from fan hub to specified radial position
0D	0-dimensional
1D	1-dimensional

2D	2-dimensional
β	Artificial mapping variable
δ	Increment in BPR
η	Isentropic efficiency
Δ	Change

SUBSCRIPTS

1	Inlet condition
13	Fan bypass exit
2	Exit condition
2D	2-D profile
21	Fan core exit
bypass	Bypass stream
core	Core stream
hub	Fan rotor hub
L	Low pressure spool
nom	Nominal
split	At bypass-core flow splitting streamline

INTRODUCTION

It is well known that the single-stage fans of high bypass ratio (typically civil) turbofan engines exhibit significant radial variations in thermodynamic variables e.g. Smith (1974). It is also apparent that there are large radial variations of flow variables exiting from the fan in low bypass ratio (typically military) turbofan engines. The layout of a typical LBPR turbofan engine is shown in Fig.(1). The average pressures and temperatures that arrive at the inlet to the engine core compressor and bypass ducts can be very different in turbofan engines due to:

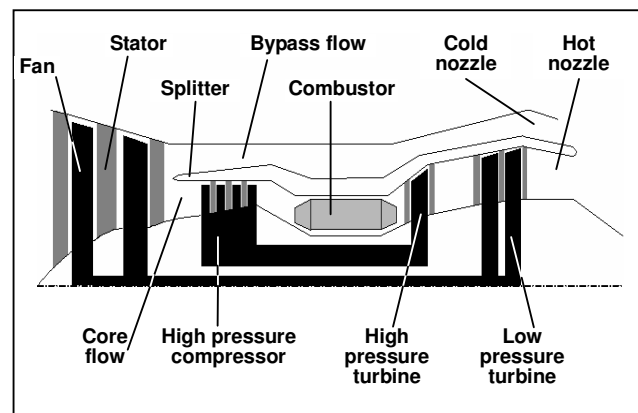


Fig.(1) Schematic of a 2-spool low bypass ratio turbofan.

1. Difference in blade speed from hub to tip
2. Designed work input variation across the blade span.
3. Viscous flow effects, particularly at the hub and tip regions.

It is necessary to firstly clarify the definitions of dimensions. The recommendations are given in NATO-RTO-TR-044 (2002). A 0D engine performance model refers to one where the components are “black boxes” and only the single values of flow parameters at component inlets and exits are computed. A 1D performance model is one where some part of the engine is modelled in more detail in another length dimension, and in this paper, the fan component is modelled in more detail in the radial dimension. A 2D performance model models the whole engine axisymmetrically, as a circumferential average. Although the engine performance model is still described as 1D, the component detail, in this case, of the fan, is 2D.

In gas turbine performance modelling, it is common practice to represent a compressor as a conventional compressor characteristic map, having single averaged values of flow or performance parameters as inputs and outputs (Kurzke, 1996). A common layout is shown in Fig.(2), with the dependent parameters being total pressure ratio (as shown) and isentropic efficiency, and the independent variables being the non-dimensional speed and beta (β), an artificial mapping parameter.

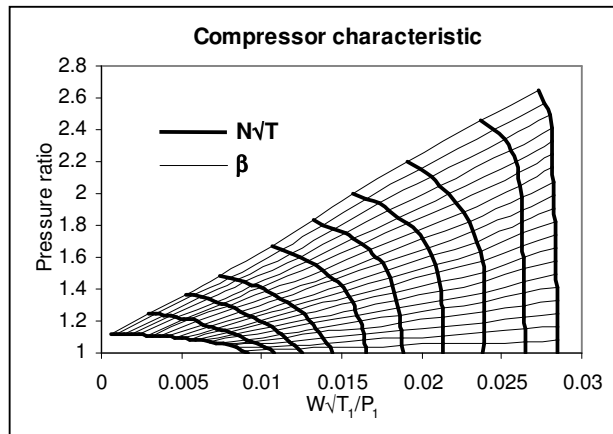


Fig.(2). Compressor characteristic map.

Recognising that a single fan characteristic providing the same single values of pressures and temperatures to the core and bypass streams would be inaccurate, the inner and outer fan model was devised as a more accurate model

Recently a 2D fan model has been developed by Yin (1999a) and the relevant techniques have also been implemented to produce a 2D fan characteristic map (Yin, 1999b). This is a more versatile procedure for modelling HBPR fans within an engine performance simulation program and is henceforth termed the 2D fan model. A similar model has been described by Riegler et al (2001).

The objective of this study is to address those cases that have been shown to occur within low bypass ratio turbofan engines where the non-dimensional overall fan characteristic map is dependent on bypass ratio (Shaw, 1982). The resulting method is a modification of the 2D fan model, and will be termed the 2D-LBPR model.

At this point, it is necessary to describe what the proposed model is intended to be used for in aero gas turbine design and research, in order to avoid confusion between this method and compressor design tools. The role is for prediction of engine performance of future engine products and for improved understanding of existing engines by analysis, typically, these performance activities would coexist with and be distinct from compressor design and analysis activities. Compressor or fan characteristic map data for these performance tools would be provided by compressor design and

research activities as a result of a combination of rig testing and compressor prediction computational tools. Therefore, for the intended role for performance, complex tools such as CFD, which are time-consuming to run and require a high level of operator skill, are inappropriate for routine, rapid performance simulation tools. During any preliminary design process, it may be required to scale up an existing engine, which involves scaling up the existing fan. It is then desired to have a simple but effective means of scaling up the current fan characteristic map. This is complicated by the nature of the existing method of modelling the fan, as described later, and the new model is intended to make this type of task more accurate. Also, the new method theoretically has an improved ability to model transient performance and so should improve the understanding of transient problems in existing engines.

The objective of this study is to implement and compare the predicted steady-state performance prediction of a hypothetical LBPR turbofan engine using three different models of the fan component, namely, the existing inner and outer fan method, the 2D fan model and the 2D-LBPR fan model. The engine studied is a two-shaft turbofan with separate nozzles as shown in Fig.(1).

BACKGROUND

The inner and outer fan model was devised to provide more realistic values of fan performance to the core and bypass streams. It has been well documented, e.g. Kurzke (1996). The two characteristics are obtained from a fan rig test procedure. When a turbofan is throttled back, the flow capacity of the first core compressor reduces more quickly than the bypass nozzle flow capacity. This results in an increase of bypass ratio when reducing speed along the working line of the fan. A nominal bypass ratio schedule dependent on non-dimensional speed is calculated with a performance simulation model: $BPR_{nom} = f(N/\sqrt{T_1})$, and the rig test is then performed following this schedule. The fan rig delivers airflow to two streams in which throttle valves are situated and can be varied separately. The following is the procedure.

1. At each speed, bypass & core throttles are adjusted so the fan operating point is on the nominal working line at the nominal bypass ratio according to the above schedule that had been pre-calculated.
2. Core mass flow is fixed at the working line value and then the bypass throttle is adjusted to change bypass mass flow incrementally from choke to stall whilst maintaining the core flow at the working line. This enables the bypass or outer fan characteristic to be obtained, (measured at bypass duct entry).
3. The bypass mass flow is then fixed at the working line value given by the nominal bypass ratio for the relevant speed, and then the core throttle is adjusted to change the core mass flow incrementally from choke to stall whilst maintaining the bypass flow at the working line. This results in the core or inner fan characteristic (measured at core entry).

Fig.(3) shows a typical inner and outer fan scheme with dependent variables as functions of the dependent variables. Pressure ratio can be used instead of $\Delta H/T$. Other variations of this scheme exist, as described by Kurzke (1996) and Marshall (1998). The use of inner and outer fan maps in this manner limits the applicability of the two characteristics to the bypass ratio schedule at which they were tested. Thus, a $BPR_{nom} = f(N/\sqrt{T_1})$ schedule refers to one fixed geometry. The model is accurate unless the gas turbine is run at a deviation from the schedule. This can be a change in geometry (altered exit throttle areas), a power offtake, bleed, engine deterioration or transient manoeuvres (Riegler et al, 2001). For example, the effect of decreasing the bypass nozzle exit area is to move the working line on the overall fan pressure ratio flow characteristic towards the surge line. A new combination of inner and outer fan maps based on a new bypass ratio schedule would be required for this new model. This is because the nominal flow split streamline has changed and now defines two compressors that are different from before.

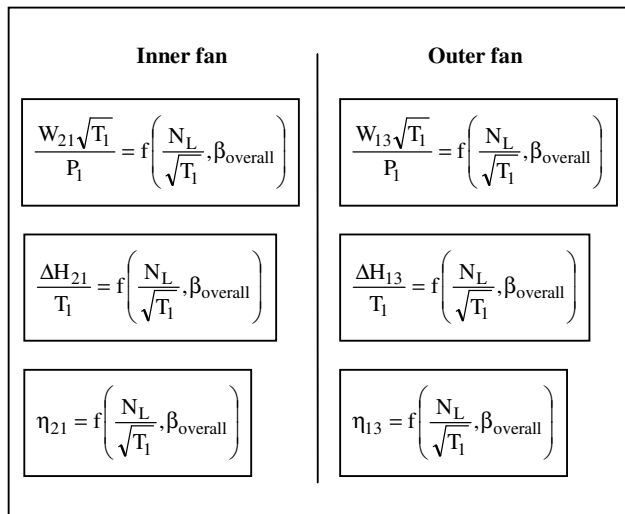


Fig.(3) Typical inner and outer scheme for low bypass fan.

The recent 2D fan model (Yin, 1999a) uses directly the profiles of thermodynamic parameters of the flow at the fan rotor exit station in modelling high bypass ratio turbofans. Fig.(4) presents the concept of the 2D fan model. Given a fan non-dimensional speed and β in the iteration scheme, the 2D fan model produces the profiles of dependent parameters at the fan exit by interpolating from stored profiles derived directly from the fan rig test. The profiles are then split according to the bypass ratio in accordance with the mass flow profile, and the resulting inner and outer

portions of the fan exit profiles are integrated to the single 1D values for the core and bypass streams respectively.

The 2D fan model is based on the following assumptions. When integrating over the whole radius, the averaged parameters like pressure ratio and fan work for the 2D fan model remain the same as those of the overall conventional fan characteristic performance maps. Also, radial profiles at the fan rotor inlet are uniform. This suggests that the profiles at the exit of the fan rotor are unaffected by the way in which the flow is split downstream to the core and bypass streams, i.e., the profiles are independent of bypass ratio at a given non-dimensional speed and fan β . This behaviour has been discussed by Riegler et al (2001), the explanation being that the bend of the split flow streamline to separate core and bypass flows occurs near the splitter, with the streamline positions through the fan staying in the same position, hence giving unaffected fan exit profiles. This was suggested to apply to low bypass ratio turbofans with the splitter far downstream of the last fan stator (Riegler et al, 2001).

Examination of rig test data of several LBPR fans by the authors suggest that the conclusion of independence of profiles of BPR is much less clear than for HBPR fans as shown by Marshall, (1998). In addition, it is well documented that some fans exist that do have a large dependency on bypass ratio, e.g. the Pratt and Whitney F100 (Shaw, 1982), Pratt and Whitney TF30-P-3 (Mazzawy, 1977), see Fig.(5). One of the reasons for the BPR dependency appears to be the effect of the proximity of the splitter on the flow within the fan. In the case of the F100, a splitter located very close to the fan exit stator causes the split flow streamline bend to occur within the fan itself, in this case, as far upstream as within the last fan rotor. This means that the work applied to the fan flow differs depending on the bypass ratio even if non-dimensional speed and β are fixed.

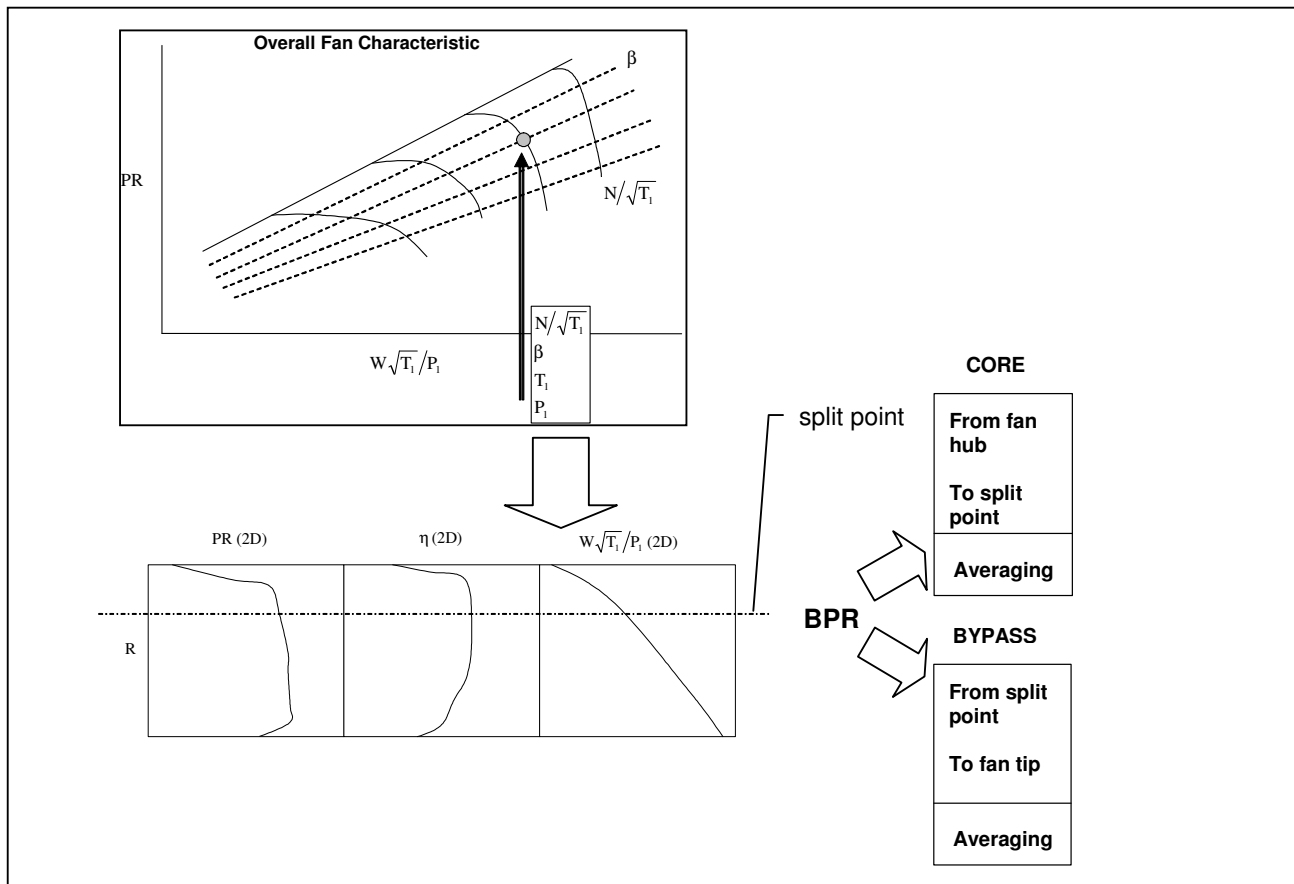


Fig.(4). 2D fan model concept.

To account for these effects, a more rigorous simulation scheme would include calculating the altered performance of the fan at different BPRs.

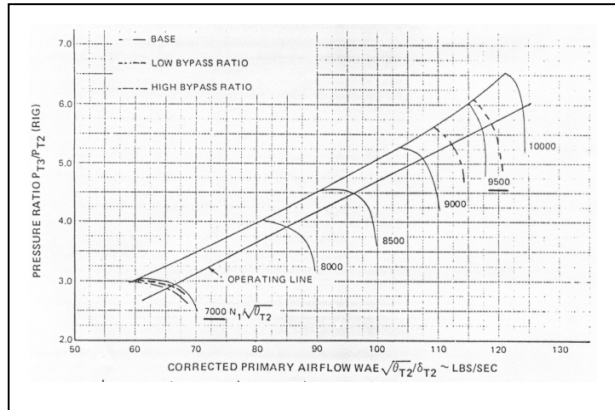


Fig.(5). Dependency of fan characteristic on bypass ratio for TF30-P-3 fan (Mazzawy, 1977).

The authors therefore modified the 2D fan model to include profiles at different BPRs, known as the 2D-LBPR model. The model is shown in Fig.(6). The major difference from the 2D fan model is that selecting β and $N_L/\sqrt{T_1}$ with the additional independent parameter BPR gives the fan profiles for the operating condition. It is immediately apparent that such a model would require a vast quantity of rig test data at all the increments of BPR (shown as δ in the diagram). It has been remarked (Riegler et al, 2001) that such testing is costly and is hardly ever performed. The authors are currently studying a method to predict the profiles at fan exit depending on the BPR based on limited test data. Nevertheless, the 2D-LBPR model depends on knowledge of the fan exit profiles at

all BPRs of interest. The profiles extracted for the given operating point are split and averaged as for the 2D fan model.

DESCRIPTION OF THE FAN MODELS

The objective of this study is to make a preliminary analysis of the effect of profiles on LBPR engine performance through three fan performance models. First is the inner and outer fan model with two conventional compressor performance characteristic maps; the inner map representing the flow for the core flow and the outer map representing the bypass flow stream of the turbofan. Second is the 2D fan model, a representation of the fan component containing information of the radial flow profiles aimed at modelling HBPR fans. Third is the 2D-LBPR fan model, a modification of the 2D fan that accounts for changed performance at different bypass ratios.

The engine chosen was a hypothetical 2-spool separate exhaust turbofan. The fan data was derived from a real LBPR fan rig test. The reason was to assess whether LBPR rig test data could be used in flow profile fan performance methods. The design points chosen as shown in Table (1) are not the same as the actual values of the fan. To make the comparisons between the models meaningful, it was important to start from the same information. The fan rig test data gave the profile data for the 2D fan and for the 2D-LBPR fan, the 'nominal' characteristic, described below, uses the same rig test data. For other BPRs, data was not available and hypothetical profiles were generated for these conditions. The inner and outer fan map then uses fan characteristic information derived from the 2D-LBPR model. A typical rig test total pressure ratio profile is shown in Fig.(7). Higher the fan rotational speed gives larger fan pressure ratio. Due to viscous effects, the pressure ratio near the hub and casing reduces. The three different fan models were incorporated into a low bypass ratio turbofan performance simulation model so that a performance prediction comparison could be carried out.

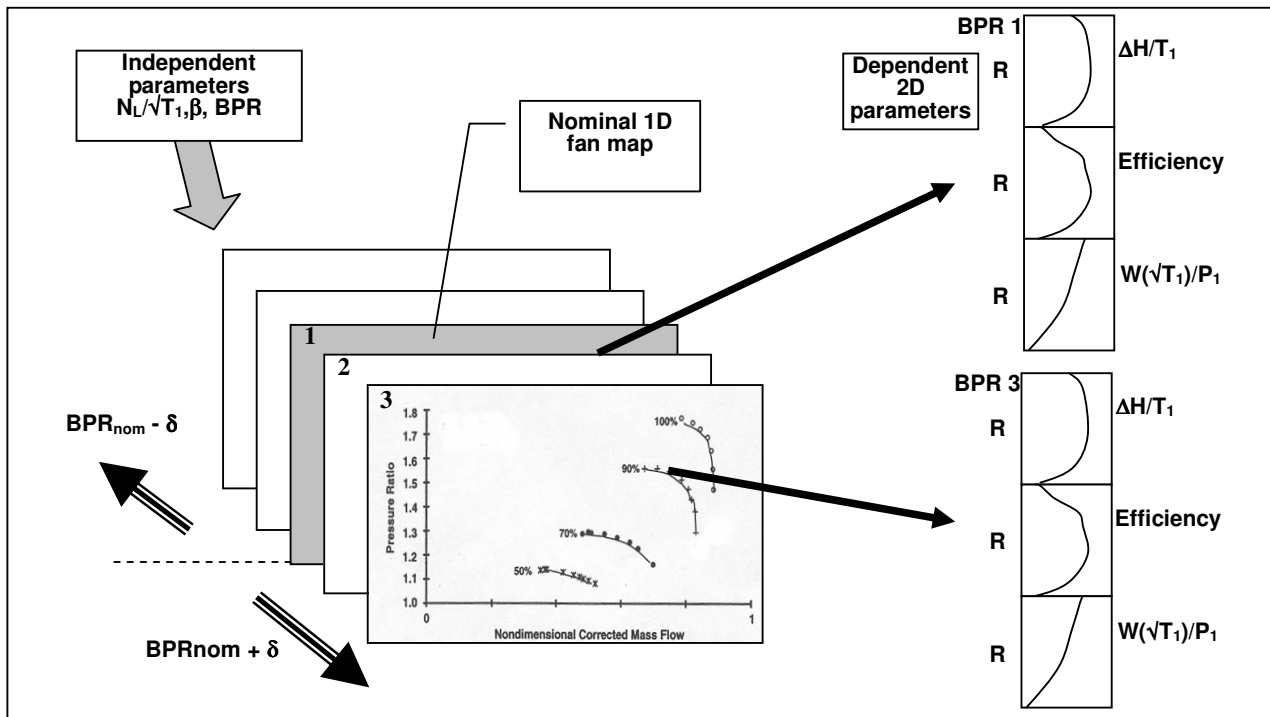


Fig.(6). 2D-LBPR fan model concept.

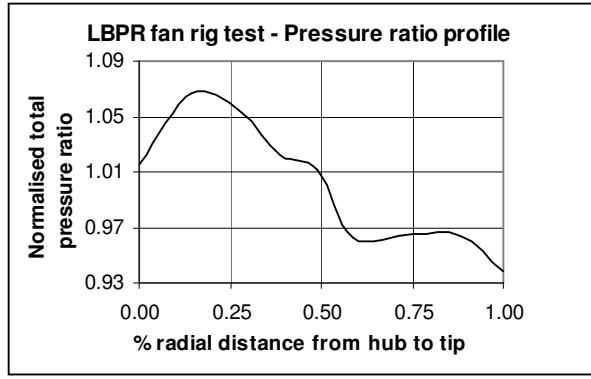


Fig.(7). Rig test total pressure profile.

Inner and outer fan model

The inner and outer fan map scheme is shown in Fig.(3). The profiles from the LBPR fan rig test in conjunction with the authors' generated profiles for the 2D-LBPR model are used to generate the two maps according to a nominal schedule of bypass ratio versus $N_t/\sqrt{T_1}$. This schedule was obtained by the result of the performance calculation of the 2D-LBPR fan model. In this way, it is known that the inner and outer model will apply to the same engine and fan geometry as for the 2D-LBPR fan model. The map is produced in the following manner. Firstly, the radial position at the fan rotor outlet of the streamline at which the fan flow splits into two streams is estimated from the mass flow profile using the nominal BPR value for the speed in question. Next, the flow properties are integrated radially and averaged for the two streams shown in Eqs.(1-6); from the split point to the tip for the bypass flow and from the split point to the hub for the core flow. This process is repeated for each intersection of β line with all the quasi-non-dimensional speed lines, denoted as β points. The averaging of each stream results in the creation of two complete compressor performance maps shown in Figs. (8a) and (8b); for the inner core stream and one for the outer bypass stream respectively. Each β point corresponds to a different flow profile.

$$W_{\text{bypass}} = W_{R_{s,\text{tip}}} - W_{R_{s,\text{split}}} \quad (1)$$

$$W_{\text{core}} = W_{R_{s,\text{split}}} \quad (2)$$

$$PR_{\text{bypass}} = \frac{1}{W_{\text{bypass}}} \int_{R_{s,\text{split}}}^{R_{s,\text{tip}}} PR_{2D} dW \quad (3)$$

$$\eta_{\text{bypass}} = \frac{1}{W_{\text{bypass}}} \int_{R_{s,\text{split}}}^{R_{s,\text{tip}}} \eta_{2D} dW \quad (4)$$

$$PR_{\text{core}} = \frac{1}{W_{\text{core}}} \int_{R_{s,\text{hub}}}^{R_{s,\text{split}}} PR_{2D} dW \quad (5)$$

$$\eta_{\text{core}} = \frac{1}{W_{\text{core}}} \int_{R_{s,\text{hub}}}^{R_{s,\text{split}}} \eta_{2D} dW \quad (6)$$

2D fan model

The 2D radial profiles of quasi-non-dimensional mass flow $W\sqrt{T_1}/P_1$, pressure ratio, PR, and isentropic efficiency, η , are a function of quasi-non-dimensional shaft speed $N_t/\sqrt{T_1}$ and β as shown in Fig.(4), and are given at the exit of the final fan stator across the annulus, with the flow assumed to be axisymmetric. The rig test data of flow at different circumferential positions have been averaged to give the representative radial profiles. At this point, an

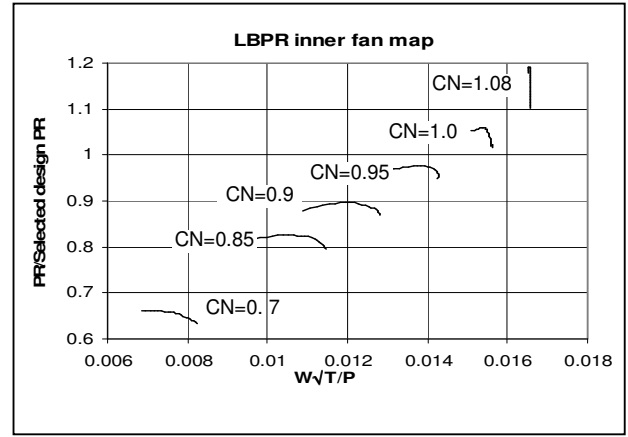


Fig.(8a). LBPR inner fan map derived from 2D-LBPR fan map.

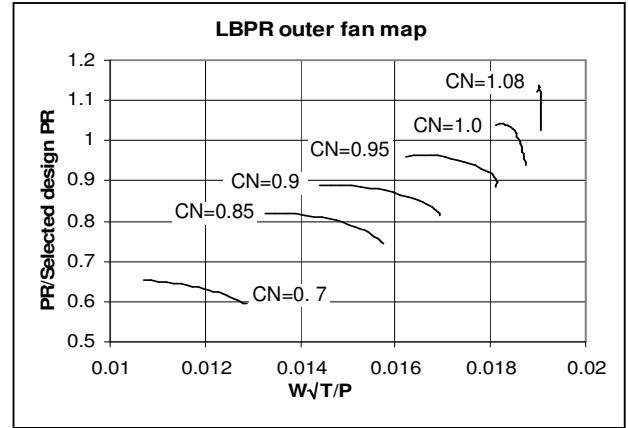


Fig.(8b). LBPR outer fan map derived from 2D-LBPR fan map.

arbitrary guess is made of the radial position at which the splitting streamline passes at the rotor exit. This effectively determines the BPR and enables the calculation of the core and bypass stream characteristics. As in a traditional model, the choice of the splitting radius is then examined relative to the mass flow capability of components downstream, in this case the bypass nozzle. The results of the calculation are compared to the choice of the radial split point. The radial split point is moved and the calculation is repeated until convergence is obtained.

The weighted averaged single values of airflow properties for the core and bypass passages downstream can then be calculated and different averaging techniques could be used in the 2D fan model to obtain these properties (Pianko et al, 1983). The rest of the calculations of the turbofan performance model are similar to a conventional simulation with the remaining components represented by component models as in a 0D performance simulation.

2D-LBPR model

Fig.(6) shows the scheme for this model. It can be seen that there is a base map termed the nominal map from which the other maps are increments in the BPR. The ideal case is for the base map to be at a single BPR, and other maps to be increments above and below this BPR. It is also possible in the model for the nominal map to have speed lines with increasing BPR as the speed decreases, with each speed line at a single BPR. The latter case has been chosen for this study. The nominal fan map is chosen to be the same as the 2D fan map data with each speed line corresponding to the BPR from the result of the 2D fan map performance calculation. With the 2D fan being independent of BPR, it was therefore necessary to assume

that all the β points on a speed line in the nominal 2D-LBPR map were at the same BPR. In reality, during the fan rig test, the different points on the speed lines have different BPRs as a result of the process of generating the inner and outer maps as described earlier. For 2D-LBPR maps at increments of the nominal BPRs, since no data was available, the authors generated new profiles to match new arbitrary 1D characteristics shown in Fig.(9).

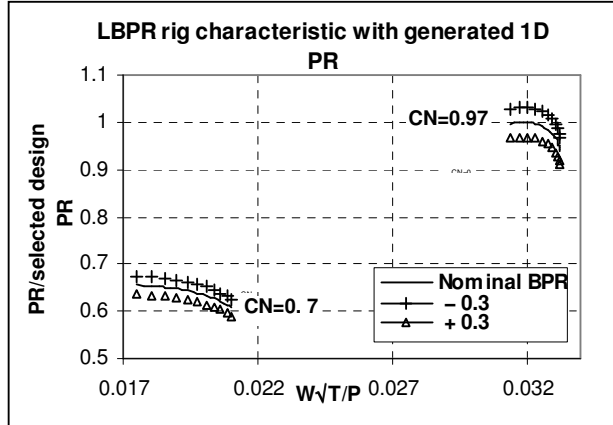


Fig.(9). Generated pressure ratio characteristic for new bypass ratios.

Some guidelines to producing the profiles were taken approximately from Fig.(5). The deviation from the nominal characteristic varied according to the non-dimensional speed and whether it was an increase or decrease of BPR. For this study, quasi-non-dimensional mass flow was not changed for the change in BPR, although the simulation scheme can accommodate this.

Engine simulation model

The three fan models described above are integrated into an aero-engine performance simulation model. A conventional iterative performance calculation code was produced. It is a typical 0D gas turbine simulation code based on the matching of flow and work compatibility between components. This code treats all of the engine components such as compressors, turbines, combustor, intake and nozzles with “black box” performance representations, having single values of flow properties at component inlet and exit. The only component of higher fidelity is the fan. In all three cases of fan model, the fan was simulated with the same components for the rest of the engine, with the same scaling factors applied in all cases to achieve design point before the calculation of off-design performance. Table(1) shows the parameters of the engine cycle.

Table(1). Turbofan cycle parameters.

Bypass Ratio	1.2
Fan Pressure Ratio	2.6
HPC Pressure Ratio	5.8
Mass Flow	110 kg/s

Steady-state performance calculations were performed using TET as the handle for the sea-level static condition. All three engines with the different fan models were calculated with fixed cold and hot nozzle exit areas. The engines with inner and outer and 2D-LBPR fan models were then compared after a 10% increase in hot nozzle area. The effect of this is to move the fan operating point to a new steady-state condition.

RESULTS AND COMPARISON

Figs.(10a-10d) show the comparison between off-design performance of a LBPR turbofan engine with the above described

inner and outer, 2D, and 2D-LBPR fan models using TET as the handle. All three models give the same result. The 2D fan had been

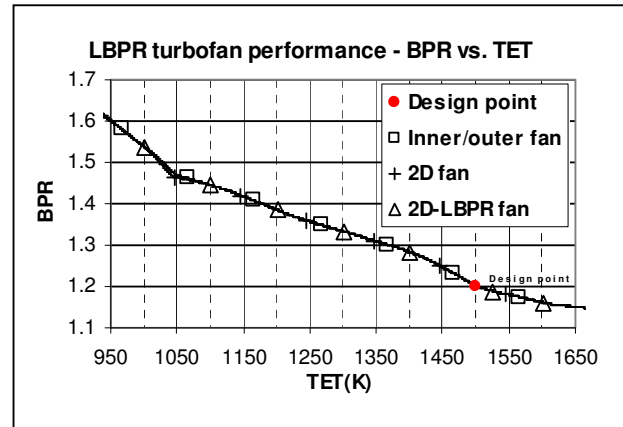


Fig.(10a). BPR vs. TET comparison for engine with different fan models, steady-state, SLS.

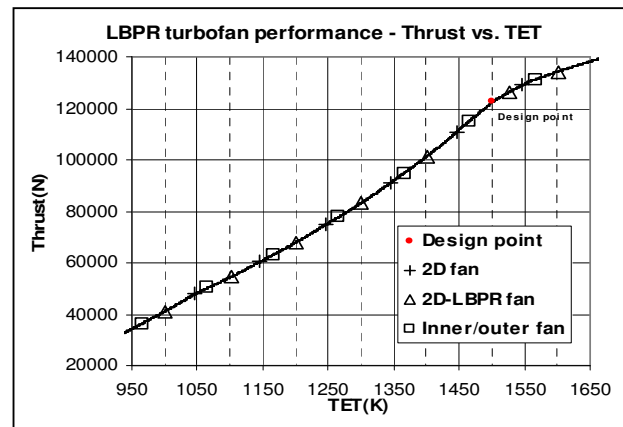


Fig.(10b). Thrust vs. TET comparison for engine with different fan models, steady-state, SLS.

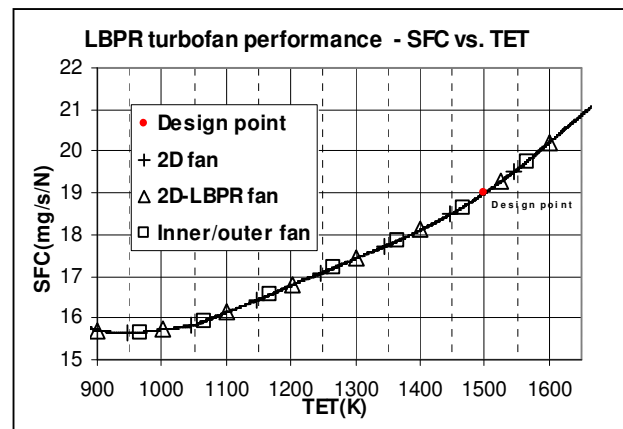


Fig.(10c). SFC vs. TET comparison for engine with different fan models, steady-state, SLS.

run to give a nominal curve of BPR vs. $N_1/\sqrt{T_1}$. The 2D-LBPR fan was generated using this nominal BPR vs. $N_1/\sqrt{T_1}$ and the 2D fan data from the rig test in the scheme given in Fig.(6). Therefore,

running it in an engine with the same nozzle areas at which the 2D fan was run will give the same result. This gives confidence that the iteration procedure in the 2D-LBPR model works correctly to calculate the correct performance, eventually selecting the correct BPR after using the other BPR maps during the iterative calculation. Furthermore, it also suggests that it is possible to use LBPR fan rig data within 2D fan-type methods directly taking the raw data and smoothing the profiles before adding β lines.

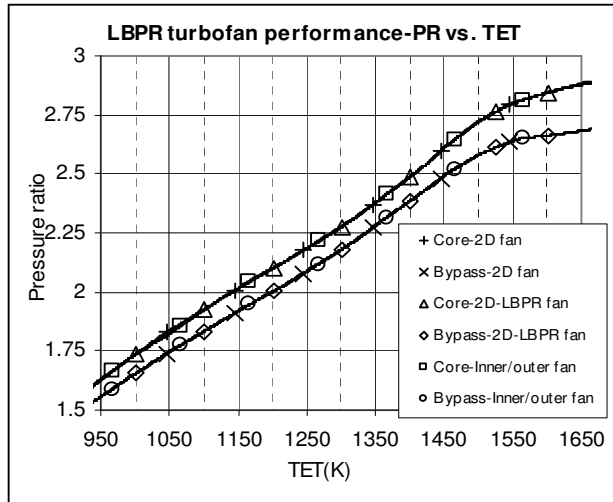


Fig.(10d). PR vs. TET comparison for engine with different fan models, steady-state, SLS.

The BPR vs. $N_1/\sqrt{T_1}$ schedule of the resulting fan working line from the 2D-LBPR off-design results is used to extract inner and outer maps from the 2D-LBPR fan data set. This resulting inner and outer fan map data run in the engine with the same nozzle areas as the 2D-LBPR fan gives the same result. This then gives confidence that it is possible to replace the inner and outer fan with the 2D-LBPR method. Fig.(10d) confirms that the inner and outer fans supply the same parameters respectively to the core and bypass streams as the 2D-LBPR fan model.

Having confirmed the ability of the 2D-LBPR fan to give the same result as the inner and outer fan when using the same geometry of the engine, a change was made to force the fan to work at a different BPR vs. $N_1/\sqrt{T_1}$ relationship by making a change in hot nozzle area. The inner and outer and 2D-LBPR models are then

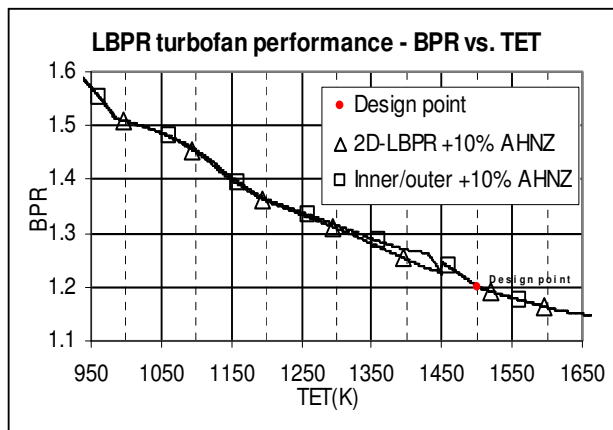


Fig.(11a). BPR vs. TET comparison for engine with 2D-LBPR and inner and outer fan models with 10% hot nozzle area increase at 1450K downwards, steady-state, SLS.

compared. The off-design calculations are again with decreasing TET as the handle, shown in Figs.(11a-11d). The hot nozzle area is altered from the setting for the previous results at 1450K downwards.

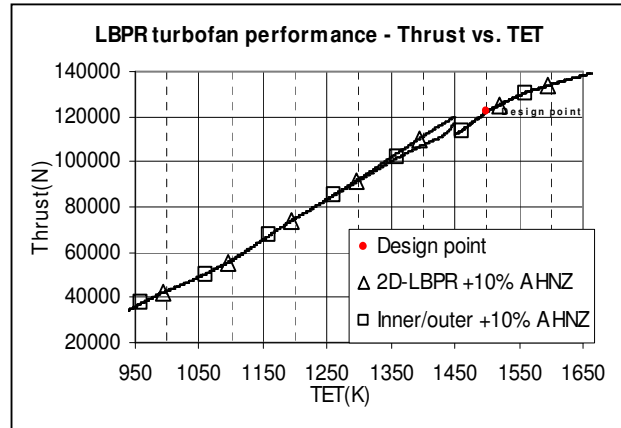


Fig.(11b). Thrust vs. TET comparison for engine with 2D-LBPR and inner and outer fan models with 10% hot nozzle area increase at 1450K downwards, steady-state, SLS.

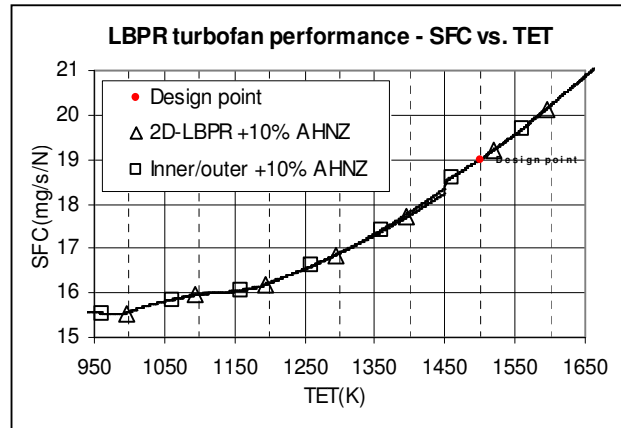


Fig.(11c). SFC vs. TET comparison for engine with 2D-LBPR and inner and outer fan models with 10% hot nozzle area increase at 1450K downwards, steady-state, SLS.

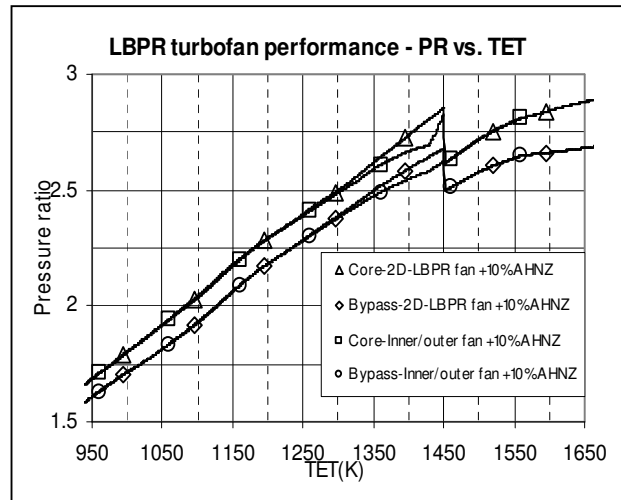


Fig.(11d). PR vs. TET comparison for engine with 2D-LBPR and inner and outer fan models with 10% hot nozzle area increase at 1450K downwards, steady-state, SLS.

As expected, the performance of the two models is the same until the area change, when the BPR vs. $N_1/\sqrt{T_1}$ relationship is altered. The inner and outer fan maps applied only to the previous relationship and so will give an incorrect performance prediction. The 2D-LBPR model should be able to account for the changes in BPR with power setting and give a different result. It should be noted that the actual results that are calculated are dependent on the authors' arbitrarily generated profiles at different BPRs, which may not be the same as the actual fan. However, the model will give the capability of a better performance prediction if the real profiles are available from rig test or able to be computed with sufficient accuracy by flow prediction methods.

CONCLUSIONS

A new performance representation of the fan component in a low bypass ratio turbofan engine has been devised: the 2D-LBPR fan which takes into account the dependency of fan performance on BPR at a given non-dimensional speed and β . The model has been compared with the existing inner and outer fan method by simulating two turbofan engines with separated exhausts in which only the fan representation is different.

Both models give the same result when run with the same relationship between BPR and power setting. When the relationship between BPR and power setting is altered, such as by a nozzle area change, the inner and outer fan model cannot take this into account without the input of a new set of compressor maps. The 2D-LBPR model can accommodate changes in bypass ratio arising from changes in geometry, transient conditions and other effects without changes. The difference in performance in this study will depend on the way in which the authors have generated the new performance maps for different BPRs for the 2D-LBPR model.

The 2D-LBPR, therefore, is a more general model that could be used independently of a fixed relationship between bypass ratio and power setting for LBPR turbofan aero engines. The benefits of using the 2D fan model is to reduce the work-load that is required to model changes in BPR by using the same 2D profile data for different geometries. No new rig testing would be required for example, for changes in bypass nozzle area, given that the same turbomachinery is retained. It is also the case that during engine development programs, scaling of the fan can be easily accommodated by a scaling of the fan exit profiles.

However, the disadvantage is the need for more expensive fan rig test data at different BPRs. The way forward could be to use a limited quantity of data in tandem with a flow prediction method to obtain the required profile data.

REFERENCES

- Kurzke, J. (1996). How to get component maps for aircraft gas turbine performance calculations. *International Gas Turbine and Aeroengine Congress & Exhibition*, Paper 96-GT-164, Birmingham, UK, June 10-13, 1996.
- Marshall, C. D. (1998). The modelling of high bypass ratio turbofans. MSc thesis, Cranfield University, School of Mechanical Engineering, September 1998.
- Mazzawy, R. S., Banks, G. A. (1977) Circumferential distortion modelling of the TF30-P-3 compression system. NASA CR-135124, 1977.
- NATO RTO-TR-044, (2002). Performance prediction and simulation of gas turbine engine operation. RTO Technical Report 44.
- Pianko, M., Wazelt, F. (1983). Propulsion and energetics panel working group 14 on suitable averaging techniques in non-uniform internal flows. AGARD advisory report No. 182 (AGARD-AR-182).
- Riegler, C., Bauer, M. Kurzke, J. (2001). Some aspects of modelling compressor behavior in gas turbine performance calculations. *Transactions of the ASME, Journal of engineering for gas turbines and power*, vol. 123, 372-378.
- Shaw, M., Murdoch, R.W. (1982). Computer modelling of

fan-exit-splitter spacing effects on F100 response to distortion, NASA CR-167879.

Smith, Jr., L. H. (1974). Some aerodynamic design considerations for high bypass ratio fans. In: *2nd International Symposium on Air Breathing Engines*, 1974, Sheffield, UK.

Yin, J. (1999a). "High Bypass Ratio Fan Modelling (WP2)", Performance Engineering UTC Annual Review Report, School of Mechanical Engineering, Cranfield University.

Yin, J. (1999b). "Proposed Calculation Procedures for the Generation and Application of 2-D Fan Characteristics", Performance Engineering UTC Document PE005. Version 2, School of Mechanical Engineering, Cranfield University.